

Conditional expectation via compact kernels

Suddhasattwa Das*

June 21, 2023

Abstract

The separate tasks of denoising, conditional expectation and manifold learning can often be posed in a common setting of finding the conditional expectations arising from a product of two random variables. This paper focuses on this more general problem and describes an operator theoretic approach to estimating the conditional expectation. Kernel integral operators are used as a compactification tool, to set up the estimation problem as a linear inverse problem in a reproducing kernel Hilbert space. This equation is shown to have solutions that are stable to numerical approximation, thus guaranteeing the convergence of data-driven implementations. The overall technique is easy to implement, and their successful application to some real-world problems are also shown.

MSC 2020 classification : 46E27, 46E22, 62G07, 62G05

Keywords : Markov kernel, statistical denoising, compact operators, RKHS

1 Introduction.

In many experiments, due to the uncertainty in the parameters of the setup, the outcome is usually to be interpreted as a conditional expectation. This is owing to the fact that the outcome which is measured is the “typical” or expected outcome, conditional on the prevailing parameters. This notion of conditional expectation has different interpretations in various contexts, such as mean-curves, least square fitting, and denoising. We present an operator theoretic approach to the problem of finding conditional expectation, which also provides robust technique for denoising. The techniques uses ideas from both kernel mean embedding as well as kernel-based operator compactification. It has an easy adaptation to be data-driven, which we also prove is convergent in the limit of large data.

To give our discussion a more firm mathematical footing we make the following assumption :

Assumption 1. *There are spaces (X, Σ_X) and (Y, Σ_Y) , and a probability measure μ on the product space $(X \times Y, \Sigma_X \times \Sigma_Y)$. Moreover, μ_X has compact support where μ_X and μ_Y are the marginals of μ on X and Y respectively.*

We interpret X as the space being directly observed, and Y to be the space from which a random input or parameter is drawn. We shall call The observation is via the following function :

Assumption 2. *There is an unknown function $f \in X \times Y \rightarrow \mathbb{R}$ which lies in the space $C(X; L^\infty(\mu_Y))$.*

The goal now is to evaluate the conditional expectation :

$$\bar{f} \in C^1(X), \quad \bar{f}(x) := \int f(x, y) d\mu(y|x). \quad (1)$$

We next recollect a few common mathematical tasks which arise from the setting of Assumptions 1 and 2.

*Department of Mathematics and Statistics, Texas Tech University, Texas, USA

Examples. The situation described in Assumptions 1 and 2 occurs commonly in many situations.

1. Additive noise : Consider the situation where \bar{f} is a random variable (r.v.) on X , $Y = \mathbb{R}^p$ endowed with a zero mean distribution μ_Y , and $f(x, y) = \bar{f}(x) + y$ is a contamination of \bar{f} with noise y . Let the product space $X \times Y$ be endowed with the product measure $\mu = \mu_X \times \mu_Y$. Then the task of denoising is about recovering \bar{f} , which is related to f and μ via (1).
2. Conditional expectation : Suppose $(\Omega, \tilde{\mu})$ is a probability measure, and $A : \Omega \rightarrow X$ and $B : \Omega \rightarrow Y$ are two random variables. Set $\mu = (A \times B)_* \tilde{\mu}$, the push forward of $\tilde{\mu}$ onto $X \times Y$. Now consider any function $f : X \times Y \rightarrow \mathbb{R}$. Then

$$(\mathbb{E}_{X} f) \circ A = \mathbb{E}(f \circ (A \times B) | A)$$

Thus the conditional expectation from (1) pulls back to an equality of random variables. This situation is the focus of the *input model uncertainty* -problem in statistics. The two r.v.-s A, B represent subsystems of the larger system Ω , and f is a statistic depending on the outcomes of A and B . Then $\mathbb{E}(f \circ (A \times B) | A)$ can be interpreted to be the mean value of the statistic f , as the input parameter B is varied.

3. Manifold learning : The notion of principal curves and manifolds are used to describe formulate manifold learning within a statistical context. Principal curves capture the notion of a curve passing through the center of a distribution. There is no unique definition, and the definition most commonly used defines this “central” curve as saddle points of the mean-squared projection distance. A commonly used definition is that of an expectation minimizing function from a manifold M . This interpretation fits well with Assumptions 1 and 2.

In Section 4 we investigate a few real world manifestations of these above scenarios, using the theoretical and numerical tools that we build. The partial integration in (1) is also called *spatial regression*. Despite its importance in several applications, robust estimation techniques are yet to be fully explored. We next try to understand the challenges associated to this task.

Challenges. There are multiple objectives one needs to be careful about in any such technique :

- (i) Smoothness : the estimated conditional expectation function preferably has some degree of regularity.
- (ii) Consistency : the outcome of the estimation technique should converge to the truth with more data.
- (iii) Data-driven : ideally the technique should not assume any prior distribution.
- (iv) Robustness : The techniques should have some robustness to random error from sources other than the probability space μ .

There has been several important paradigms developed to address this estimation problem, but most of them lack in addressing one or more out of the above four objectives. We now take a brief look at these.

Related work. While Assumptions 1 and 2 describe a basic scenario in many theoretical and real-world situations, they do not provide a recipe for estimating \bar{f} from (1). There has been several ideas proposed, which we organize into five classes. Nearest-neighbor based techniques [e.g. 1, 2, 3] are data-driven and easily scalable with large data, but lack a framework to guarantee consistency. The idea is to denoise a local piece of the data cloud by taking an average of nearest neighbors, via a technique known as Non-Local-Means (NLM) [2, 3]. In spite of different weighting schemes being proposed, these techniques also suffer from the presence of bias. A second class of techniques use principal component analysis and its statistical properties [e.g. 4]. However, these techniques are framed in a set of Assumptions more restrictive than our

general case. A third important class of techniques are based on the notion of *principal curves* [e.g. 5]. Here, the target function is set to be a curve passing through the middle of a distribution. One then uses any of the vast number of gradient-descent-based to minimize the squared divergence from the mean curve. Principal curve estimation techniques come with all the advantages and disadvantages of gradient-descent learning, and also lack a firm footing in probabilistic assumption. A fourth class of techniques rely on concepts from traditional Harmonic analysis. The most notable is a technique named *conditional mean embedding* [6], which sets up the estimation as a linear-algebraic concept. The other most common practice [e.g. 7, 8] is to assume a hypothesis space, and a noise prior on the coefficients with respect to a basis or frame.

Our proposed technique falls under a fifth class of techniques - kernel based methods. Several ideas have been proposed for applying kernel-based techniques to conditional expectation estimation. Some examples are the use of kernels for non-isotropic mixing spatial data [9], using local linear kernel estimators [10], or adaptation of ideas from kernel density estimation [11]. We use a combination of compactification and reproducing kernel Hilbert space theory to perform our estimation.

Outline. We describe the technical details next in Section 2. We setup the problem in a hypothesis space called reproducing kernel Hilbert space. The target function is to be determined via a linear inverse problem. To make the problem robust to finite rank approximations, we use compact operators on both sides of the equation. Readers looking for the algorithmic implementation and convergence guarantees are directed to the next Section 3. We demonstrate some applications in Section 4 and provide some discussions in Section 5.

2 The technique.

Kernel based methods offer a non-parametric approach to learning, and has been used with success in many diverse fields such as spectral analysis [12, 13], discovery of spatial patterns [e.g. 14, 15], and the discovery of periodic and chaotic components of various real world systems [e.g. 16, 17], and even abstract operator valued measures [18]. We now describe their role and understand their advantages.

Kernel. A kernel on the space X is a bivariate function $k : X \times X \rightarrow \mathbb{R}$, which is supposed to be a measure of similarity between points on X . Bivariate functions such as distance and inner-products are examples of kernels. We shall the widely used *Gaussian* kernels, defined as

$$k_{\text{Gauss},\epsilon}(x, y) := \exp\left(\frac{1}{\epsilon} \text{dist}(x, y)^2\right), \quad \forall x, y \in X.$$

Gaussian kernels have been shown to have deep connections with the geometry or topology of the underlying space [e.g. 19, 20, 21, 22, 23]. Gaussian kernels have the important property of being *strictly positive definite*, which means that given any distinct points x_1, \dots, x_N in X , numbers a_1, \dots, a_N in \mathbb{R} , the sum $\sum_{i=1}^N \sum_{j=1}^N a_i a_j k(x_i, x_j)$ is non-negative, and zero iff all the a_i -s are zero.

Closely associated to kernels are kernel integral operators (k.i.o.). Given a probability measure ν on X , one has an integral operator associated to k , defined as

$$K^\nu : L^2(\nu) \rightarrow C^r(X), \quad (K^\nu \phi)(x) := \int_X k(x, y) \phi(y) d\nu(y).$$

Here, $r \geq 0$ denotes the degree of smoothness of the kernel k on X , For this reason, k.i.o.-s are also known as smoothing operators. In fact, under mild assumptions, we shall see how k.i.o.-s embed functions in $L^2(\nu)$ into function spaces of higher regularity. Moreover, k.i.o.-s can be used to make modifications to the underlying kernel to adapt them more to the underlying space. One such modified family of kernels we are

interested in is a *diffusion* kernel, defined as

$$k_{\text{diff},\epsilon}^{\mu}(x, y) = \frac{k_{\text{Gauss},\epsilon}(x, y)}{\text{deg}_l(x) \text{deg}_r(y)}, \quad (2)$$

$$\text{deg}_r(x) := \int_X k_{\text{Gauss},\epsilon}(x, y) d\mu(y), \quad \text{deg}_l(x) := \int_X k_{\text{Gauss},\epsilon}(x, y) \frac{1}{\text{deg}_r(x)} d\mu(y).$$

Diffusion kernels have been shown to be good approximants of the local geometry in various different situations [e.g. 21, 19, 24, 25], and is a natural choice for non-parametric learning. It has the added advantage of being symmetrizable :

$$\rho(x) k_{\text{diff},\epsilon}^{\mu}(x, y) \rho(y)^{-1} = \tilde{k}_{\text{diff},\epsilon}^{\mu}(x, y) = \frac{k_{\text{Gauss},\epsilon}(x, y)}{[\text{deg}_r(x) \text{deg}_r(y) \text{deg}_l(x) \text{deg}_l(y)]^{1/2}}, \quad (3)$$

where

$$\rho(z) = \text{deg}_l(z)^{1/2} / \text{deg}_r(z)^{1/2}.$$

Symmetric kernels allow the use of tools from RKHS theory, which we briefly review next.

RKHS. A reproducing kernel Hilbert space or *RKHS* is a Hilbert space of continuous functions, in which pointwise evaluations are bounded linear functionals. Any continuous symmetric, strictly positive definite kernel k (such as (2)) induces an RKHS which contains linear sums of the form $\sum_{n=1}^N a_n k(\cdot, x_n)$, in which the inner product is given by

$$\left\langle \sum_{n=1}^N a_n k(\cdot, x_n), \sum_{m=1}^M b_m k(\cdot, y_m) \right\rangle = \sum_{n=1}^N \sum_{m=1}^M a_n^* b_m k(x_n, y_m).$$

The full details of the construction of this space \mathcal{H} can be found in any standard literature [e.g. 26]. The functions $k(\cdot, x_n)$ are called the *sections* of the kernel k . The kernel sections are members of the RKHS and span the RKHS. One of the defining properties of RKHS is the *reproducing* property :

$$\langle k(\cdot, x), f \rangle = f(x), \quad \forall x \in X, \forall f \in \mathcal{H}.$$

When an RKHS is used as the hypothesis space in a learning problem, the target function is assumed to be a finite sum $\sum_{n=1}^N a_n k(\cdot, x_n)$ of the kernel sections. Let ν be any probability measure on X , and K^ν be the kernel integration operator associated to k and ν . Then it is well known that the image of K^ν lies in \mathcal{H} , and is dense in $C(\text{supp}(\nu))$, the space of continuous functions on the support of ν . We denote this image as \mathcal{H}_ν . Let ν be a discrete measure $\nu = \sum_{n=1}^\infty w_n \delta_{x_n}$, i.e., an aggregate of Dirac-delta measures supported on discrete points x_n along with weights $w_n > 0$ which sum to 1. Then \mathcal{H}_ν is precisely the span of the kernel sections $\{k(\cdot, x_n) : n = 1, \dots, N\}$. With this in mind, we assume :

Assumption 3. *The conditional expectation \bar{f} from (1) lies in \mathcal{H}_{μ_X} .*

Note that the kernel can be of arbitrary design and thus the function \bar{f} need not lie in \mathcal{H}_{μ_X} . In spite of this, Assumption 3 makes sense from a mathematical point of view, as it provides a condition that guarantees convergence. Moreover, it is not restrictive due to the density of the RKHS in $C(X)$. Then the sequence of norms

$$a_n := \inf \left\{ \|h\| : h \in \mathcal{H}_{\mu_X}, \|f - h\|_{C(X)} < \frac{1}{n} \right\}, \quad n = 1, 2, \dots$$

is called the rate of approximation of f . Each of the RKHS approximations can be used as a candidate for f that satisfies Assumption 3. Its oscillatory nature, captured by $\|f\|_{\mathcal{H}}$, determines the tuning of the experiment parameters.

Thus, an RKHS supported on the observed data-space X will be our choice of hypothesis space in the estimation of the conditional expectation. An RKHS provides several advantages, it has a Hilbert space structure, pointwise evaluation is a bounded operation, and under mild conditions, they are dense in the space of continuous functions. More importantly, the conditional expectation operator has been shown to be well approximated in operator norm by Hilbert Schmidt operators [27]. This gives kernel-based techniques a clear edge over other techniques. Finally, RKHS in many situations can be endowed with a Banach algebra structure [28], thus enriching them further for Harmonic analysis.

A note about this assumption :

RKHS-like kernels. The kernel $\tilde{k}_{\text{diff},\epsilon}^\mu$ from (3) is clearly symmetric. Since it is built from the s.p.d. kernel $k_{\text{Gauss},\epsilon}$, $\tilde{k}_{\text{diff},\epsilon}^\mu$ is s.p.d. too and thus generates an RKHS of its own. Moreover, the kernel $k_{\text{diff},\epsilon}^\mu$ can be symmetrized by a degree function ρ , which is both bounded and bounded above 0. Such a kernel will be called *RKHS-like*. Let M_ρ be the multiplication operator with ρ . Then

$$\text{ran } K_{\text{diff},\epsilon}^\mu = \text{ran } M_\rho \circ \tilde{K}_{\text{diff},\epsilon}^\mu.$$

Again, because of the properties of ρ , both M_ρ and its inverse are bounded operators. Thus there is a bijection between the RKHS generated by $\tilde{k}_{\text{diff},\epsilon}^\mu$, and the range of the integral operator $K_{\text{diff},\epsilon}^\mu$.

The diffusion kernel has the additional property of being a Markov kernel :

$$\begin{aligned} K_{\text{diff},\epsilon}^\mu 1_X &= M_{\text{deg}_l}^{-1} K_{\text{Gauss},\epsilon}^\mu M_{\text{deg}_r}^{-1} 1_X = M_{\text{deg}_l}^{-1} K_{\text{Gauss},\epsilon}^\mu \text{deg}_r^{-1} \\ &= M_{\text{deg}_l}^{-1} \text{deg}_l = 1_X. \end{aligned}$$

Kernel smoothing. Suppose α is a probability measure on X , absolutely continuous with respect to μ_X . Then

$$\begin{aligned} \int_X \bar{f}(x) d\alpha(x) &= \int_X \int_Y f(x, y) d\mu(y|x) d\alpha(x) = \int_X \int_Y f(x, y) d\mu(y|x) \frac{d\alpha}{d\mu_X}(x) d\mu_X(x) \\ &= \int_X \int_Y f(x, y) \frac{d\alpha}{d\mu_X}(x) d\mu(y|x) d\mu_X(x) \\ &= \int_{X \times Y} \left[f(x, y) \frac{d\alpha}{d\mu_X}(x) \right] d\mu(x, y) \end{aligned}$$

Such an absolutely continuous probability measure can be realized using a Markov integral operator, built from a *Markov transition kernel* as defined below :

$$p_\delta : X \times X \rightarrow \mathbb{R}_0^+, \quad p_\delta(z, x) := \exp(-\|z - x\|^2 / \delta) / \int_X \exp(-\|z - y\|^2 / \delta) d\mu_X(y).$$

Note that for every $z \in X$, the kernel section $p_\delta(z, \cdot)$ is a non-negative function with integral equal to one. Thus it can be interpreted as a probability density. Let $\text{Prob}(X; \mu_X)$ be the collection of probability measures on X absolutely continuous with respect to μ_X .

$$\begin{array}{ccc} X & \overset{p^*}{\dashrightarrow} & L^1(\mu_X)^* \\ \downarrow p & & \uparrow \subset \\ S^1 L^1(\mu_X; \mathbb{R}_0^+) & \longrightarrow & \text{Prob}(X; \mu_X) \end{array}$$

Then we have an associated integral operator $P_\delta^{\mu_X} : L^2(\mu_X) \rightarrow C^\infty(X)$, whose action on any $\psi \in L^2(\mu_X)$ is given by

$$(P_\delta^{\mu_X} \psi)(z) := \int_X p_\delta(z, x) \psi(x) d\mu(x) = \langle p_*(z), \psi \rangle, \quad \forall z \in X.$$

This kernel p_δ on X has the following trivial extension to a transition kernel

$$q_\delta : X \times (X \times Y) \rightarrow \mathbb{R}_0^+, \quad q_\delta(z, x, y) := p_\delta(z, x).$$

This trivial extension allows us to write

$$P_\delta^{\mu_X} \bar{f} = Q_\delta^\mu f \tag{4}$$

The simple identity in (4) underlines our main idea. It is based on the compactness of integral operators.

Theorem 1. *Suppose Assumptions 1, 2 and 3 hold. Let ν, α be any probability measures on X . Then if $\phi_{\nu, N}$ is the least-squares solution in ϕ to the equation*

$$P_\delta^\alpha K^\nu \phi = Q_\delta^\alpha f \tag{5}$$

then

$$\lim_{\alpha \rightarrow \mu} \lim_{\nu \rightarrow \mu_X} \|K^\nu \phi_{\nu, N} - \bar{f}\|_{C(X)} = 0. \tag{6}$$

Under Assumptions 3 and by (4), there is an exact solution to (5) when $\alpha = \mu$ and $\nu = \mu_X$. That fact the solutions converge implies that the the equation is stable to finite rank approximation, a fact we utilize in Theorem 2 later in Section 3. The diagram in (7) illustrates our scheme.

$$\begin{array}{ccccc}
 & C(X; L_\infty(Y)) & & L^2(\mu) & \\
 & \swarrow \mathbb{E}_{\cdot, X} & \searrow Q_\delta & \nearrow j & \searrow \pi_{\delta, \nu} \\
 \mathcal{H}_\mu & & C(X) & & \text{ran}(P_\delta \iota_\nu K^\nu) \\
 & \searrow \iota_\mu & \nearrow P_\delta & \searrow A_{\delta, \nu} & \swarrow P_\delta^{-1} \\
 & L^2(\mu) & & \mathcal{H}_\nu &
 \end{array} \tag{7}$$

The blue loop expresses the identity in (4). The smoothing operator Q_δ^μ is shown as the composite of the conditional expectation operator, and the smoothing operator P_δ^μ . The map $\iota_\mu : C(X) \rightarrow L^2(\mu)$ is just the inclusion map of continuous functions in the space of square integrable functions, which is made possible by the compactness of $\text{supp}(\mu_X)$. The map $\iota_\nu : \mathcal{H}_\nu \rightarrow L^2(\nu)$ is similar inclusion map. The map

$$\pi_{\delta, \nu} : L^2(\mu) \rightarrow \text{ran}(P_\delta \iota_\nu K^\nu)$$

is an orthogonal projection which arises naturally from the least-squares problem.

The green loop in (7) represents a data-driven or finite-rank approximation of the RKHS learning. The blue loop represents the compactification scheme, which is also well approximable by data.

In the next section we look at a practical implementation of this scheme, and the accompanying guarantee of convergence.

3 Numerical implementation.

In a data-driven implementation, the inputs to any numerical recipe is a dataset, along with some algorithmic parameters. We assume that the data originates as follows :

Assumption 4. *There is a sequence of points $(x_n, y_n) \in X \times Y$ for $n = 1, 2, 3, \dots$, equidistributed with respect to the probability measure μ from Assumption 1.*

The concept of equidistribution is a major relaxation of the assumption of being i.i.d.. Such an assumption has been utilized with great success in the theoretical understanding of numerical methods for timeseries which have strong correlations, such as those arising from dynamical systems [e.g. 12, 18, 13]. Algorithm 1 below presents our main procedure.

Algorithm 1. *RKHS representation of conditional expectation.*

- **Input.** *A sequence of pairs $\{(x_n, y_n) : n = 1, \dots, N\}$ with $x_n \in \mathbb{R}^d$ and $y_n \in \mathbb{R}$.*

- **Parameters.**

1. *Choice of RKHS-like kernel $k : \mathbb{R}^d \times \mathbb{R}^d \rightarrow \mathbb{R}^+$.*
2. *Smoothing parameter $\delta > 0$.*

- **Output.** *A vector $\bar{a} = (a_1, \dots, a_N) \in \mathbb{R}^N$ such that*

$$(\mathbb{E}_{.X} f)(x) \approx \sum_{n=1}^N a_n k(x, x_n), \quad \forall x \in \mathbb{R}^d.$$

- **Steps.**

1. *Compute a Markov kernel $[P_\delta] \in \mathbb{R}^{N \times N}$ using Algorithm 4, with $\{x_n\}_{n=1}^N$ and δ as input.*
2. *Compute the kernel matrix $[K] \in \mathbb{R}^{N \times N}$, with $[K]_{i,j} = k(x_i, x_j)$.*
3. *Compute $\bar{z} = [P_\delta] \bar{y}$.*
4. *Find the least-squares solution \bar{a} to the equation $[P_\delta] [K] \bar{a} = \bar{z}$.*

Algorithm 1 has two components, the choice of an RKHS-like kernel, and the creation of a Markov kernel which approximates the smoothing operator. The latter procedure is standard and we provide it below for the sake of completion.

Algorithm 2. *Building a Markov kernel kernel.*

- **Input.** *A time series $\{x_n\}_{n=1}^N$ of points in \mathbb{R}^d , and a constant $\delta > 0$.*

- **Output.** *An $N \times N$ row-stochastic matrix $[P_\delta]$.*

- **Steps.**

1. *Compute the Gaussian kernel*

$$[G] \in \mathbb{R}^{N \times N}, \quad [G]_{i,j} = \exp\left(-\frac{1}{\delta} \|x_i - x_j\|^2\right)$$

2. *Compute*

$$\text{deg} := [G] \bar{1}_N, \quad D := \text{diag}(\text{deg}), \quad [P_\delta] = D^{-1} [G].$$

Finally, we come to the choice of the kernel k , which we set to be the diffusion kernel from (2). See Section 2 for a discussion of its RKHS-like properties.

Algorithm 3. *Building a diffusion kernel.*

- **Input.** A time series $\{x_n\}_{n=1}^N$ of points in \mathbb{R}^d , and a bandwidth parameter $\epsilon > 0$.
- **Output.** An $N \times N$ matrix $[K]$.
- **Steps.**

1. Compute the Gaussian kernel

$$[G] \in \mathbb{R}^{N \times N}, \quad [G]_{i,j} = \exp\left(-\frac{1}{\epsilon} \|x_i - x_j\|^2\right)$$

2. Compute degree vectors

$$\text{deg}_R := \frac{1}{N} [G] \vec{1}_N, \quad D_R := \text{diag}(\text{deg}_R), \quad \text{deg}_L := \frac{1}{N} [G] D_R^{-1} \vec{1}_N, \quad D_L := \text{diag}(\text{deg}_L).$$

3. Finally compute $[K] = D_L^{-1} [G] D_R^{-1}$.

Theorem 2 below provides an interpretation of the output vector \vec{a} from Algorithm 1, and the nature of the convergence of the results.

Theorem 2. Suppose Assumptions 1, 2, 3 and 4 hold. Let \vec{a} be the output of Algorithm 1 is applied to the data $(x_n, y_n)_{n=1}^N$. Then $\sum_{n=1}^N a_n k(\cdot, x_n)$ converges pointwise to $\mathbb{E}_{X,f}$.

Theorem 2 is a direct consequence of Theorem 1. Note that Theorem 2 is independent of the choice of the kernel k in Algorithm 1. Algorithm 1 itself can be carried out on any dataset (x_n, y_n) , irrespective of whether any of Assumptions 1, 2, 3 and 4 hold. Assumptions 1 and 4 are needed to place the dataset in context, and Assumptions 2 and 3 are required to guarantee their convergence.

We next apply Algorithm 1 to a few practical problems.

4 Examples.

4.1 Denoising. As explained in Section 1, denoising is a particular instance of Assumptions 1 and 2. We illustrate an application of Algorithm 1 to continuous images in Figures 1. The task of imaging discontinuous images involves many other considerations such as edge detection, and is postponed to a later study. Each of the RGB components of a continuous image may be considered to be points on the graph of a continuous map $\bar{f}: [0, 1]^2 \rightarrow \mathbb{R}$. The points correspond to the image under \bar{f} of points on a rectangular lattice within $[0, 1]^2$. The noise can be considered as an addition from a Gaussian random variable drawn from \mathbb{R} . We chose for \bar{f} the function

$$\bar{f}: [0, 1]^2 \rightarrow \mathbb{R}, \quad \bar{f}(x_1, x_2) := . \tag{8}$$

Theorem 2 states that the convergence or accuracy of the results are dependent on increasing the number of data samples. This presents as a problem in image denoising, as the number of data samples is exactly the number of pixels, and is usually fixed and limited. As a result, the outcome of the numerical procedure becomes sensitive to the smoothing parameter parameter δ and the C^1 norm of the true image.

4.2 Principal curves - electrostatic charge. Given any C^2 curve $\lambda: [0, 1] \rightarrow \mathbb{R}^+$, one can define the function

$$f: [0, 1] \times \mathbb{R} \rightarrow \mathbb{R}, \quad (x, y) \mapsto \lambda(x) + y/\rho(x), \quad \rho(x) := \frac{1}{0.01 + |f''(x)|}. \tag{9}$$

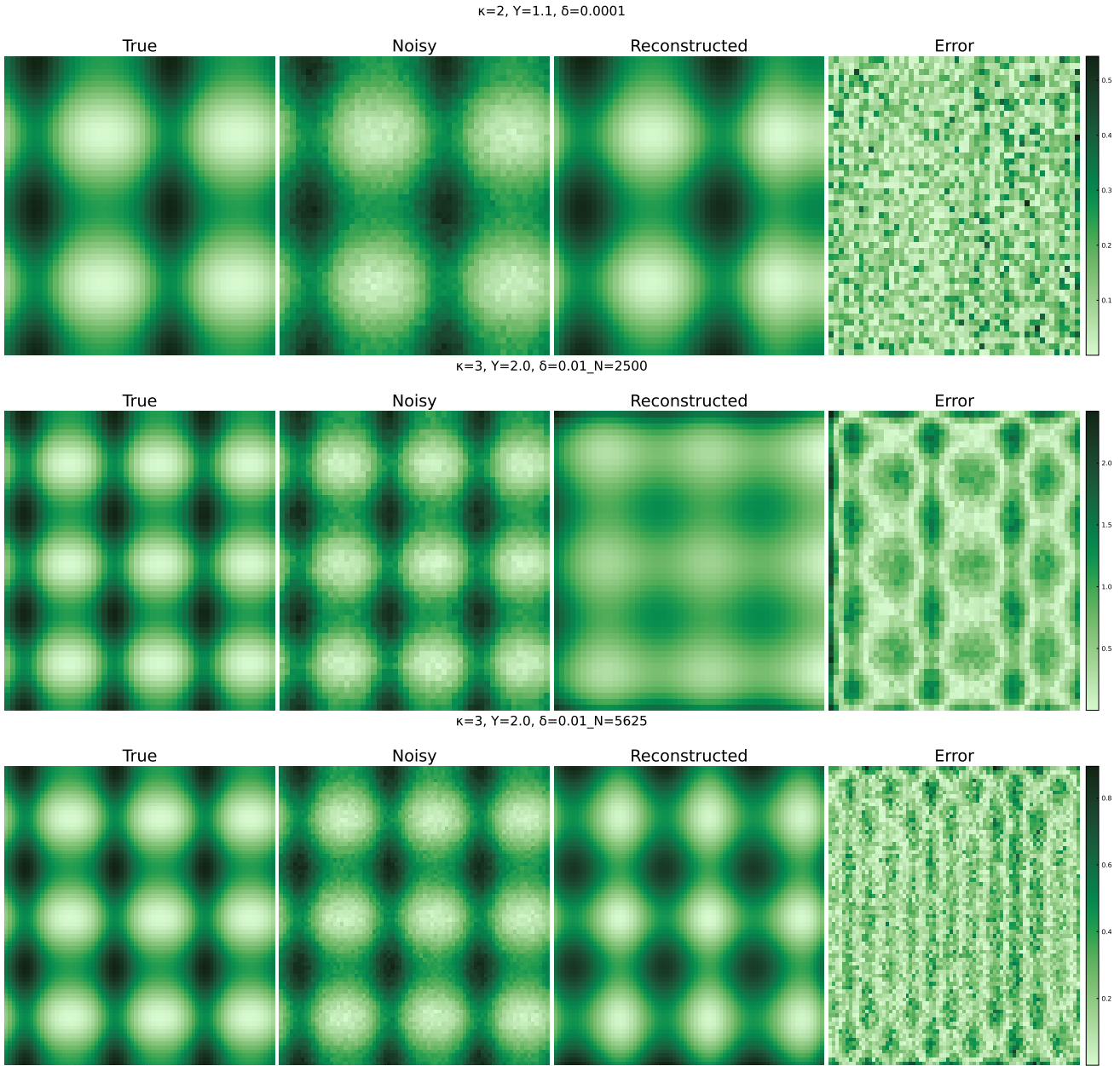


Figure 1: Denoising at fixed binning level. The figures show the results of denoising a monochromatic image, which can be expressed as a continuous function of time given by (8). The parameter κ is an index of the C^1 norm of the function. The first row shows that Algorithm 1 performs reasonably well for $\kappa = 2$ on a 50×50 pixel image, but the performance deteriorates when $\kappa = 2$. The third row shows a much improved result when the image gets more detailed with an increased size 75×75 .

Equation (9) is a simplified model of electrostatic charged distribution on curved surfaces. For our test case, we choose for λ the function

$$\lambda(x) = \exp(\sin(2\pi x)^2), \quad \forall x \in [0, 1]. \quad (10)$$

The two derivatives of λ are :

$$\begin{aligned}\lambda'(x) &= 2\pi\lambda(x)\sin(4\pi x) \\ \lambda''(x) &= 8\pi^2\lambda(x)\cos(4\pi x) + 4\pi^2\lambda(x)\sin(4\pi x)^2 \\ &= 4\pi^2\lambda(x)\left[2\cos(4\pi x) + \sin(4\pi x)^2\right] \\ &= 4\pi^2\lambda(x)\left[2 - [\cos(4\pi x) - 1]^2\right]\end{aligned}$$

Let us assign spaces and measures

$$X = [0, 1], \mu_X = \text{Leb}_{[0,1]}, Y = \mathbb{R}, \mu_Y \sim N(0, 1), \mu = \mu_X \times \mu_Y.$$

Then Algorithm 1 applied to data points distributed according to the push-forward of μ under f should yield an approximation of $\bar{f} = \mathbb{E}_X f$, which according to (9) coincides with $\bar{f} = \lambda$. Also note that $\rho(x)$, which is the standard deviation of the conditional measure $\mu(\cdot | x)$, is itself a conditional expectation, namely, $\mathbb{E}_X |f - \bar{f}|^2 = \rho$. See Figure 2 for the results of our algorithm applied to data.

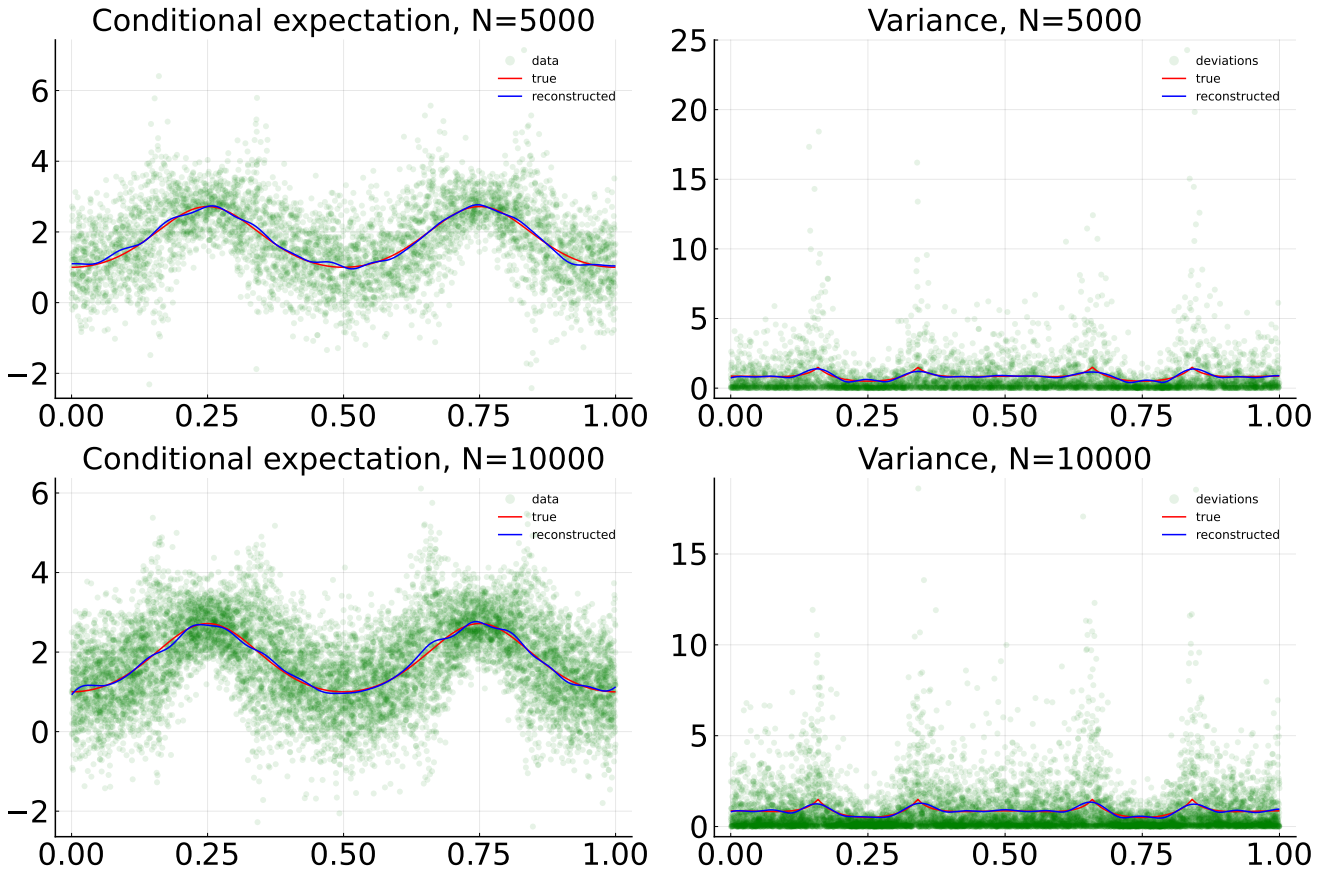


Figure 2: Principal curve estimation. Equation (9) is a realization of Assumptions 1 and 2, and presents a simplified view of electrostatic charge distribution along a wire. We assume that the function λ takes the form in (10). The left panels above show the results of applying Algorithm 1 to data equidistributed with respect to this distribution, to recover the conditional expectation as a function over $X = [0, 1]$. The results show a close match with the true mean, which is simply the curve λ . The results also visibly improve as the number of samples are increased. The right panel shows a repeated use of Algorithm 1 to reconstruct the variance as a function over $X = [0, 1]$. Again, the results show a strong match with the true function, which is ρ .

5 Conclusion.

We have presented a numerical procedure in Algorithm 1, which according to Theorem 2, provides a convergent estimate of a conditional expectation in the context of Assumptions 1–4. Theorem 2 is the data-driven version of Theorem 1, which is stated in purely operator theoretic terms. This numeric procedure may be applied to any practical problem which can be set in this context. We test our problems on two relatively simple problems from the fields of image denoising and manifold learning.

Future directions. The convergence guarantee provided in Theorems 1 and 2 ensure the accuracy of the results when the number of data samples are large enough. This also leads to several future directions of work.

1. Tuning parameter δ : The main challenge in the scheme based on (4) is to average out the effect of the Y -variable, within the integrals

$$(Q_\delta^\mu f)(z) = \int_{X \times Y} p_\delta(z, x) f(x, y) d\mu(x, y) \approx \int_{B(z, \delta')} p_\delta(z, x) \int_Y f(x, y) d\mu(y|x) d\mu_X(x).$$

Here δ' is the effective radius of integration, which goes to zero as δ goes to zero. The smaller δ is, the more number of total samples are needed so that sufficiently many of them fall within this sphere $B(z, \delta')$. Thus a larger smoothing radius δ leads to a faster convergence with N . On the other hand, a larger δ and N also increases the condition number of the matrix $[P_\delta]$, which could adversely affect the accuracy of the solutions. There is no recipe for tuning these parameters that would work uniformly well in all applications.

2. Images with limited resolution : Given a fixed resolution for an image, say $m \times n$ pixels, one would be limited to $N = mn$ data samples, as each pixel would correspond to a data point x_n drawn uniformly from the unit square. As seen in Figure 1, this could lead to a deterioration in performance as the image function becomes more oscillatory. A remedy is to first increase the resolution of the image using the capability of RKHS for accurate out-of-sample evaluations. This would be the subject of a more thorough and focused study in a subsequent work.
3. Subsampling : While it is desirable to use all available data samples when approximating Q_δ , one has the flexibility of choosing a subset of the data-points for approximating K^μ , as this is an integral operator on the lower dimensional space X . As long as the condition that the subsampling measure ν converges weakly to μ , any subsampling strategy would suffice.
4. Choice of kernel : The question of which kernel would be optimal in a learning problem has been a long standing question, with no clear and unique answer [e.g. 29, 30, 31]. While we have explained the reason behind our choice of using diffusion kernels, various other adaptive kernels could be good candidates, such as variable bandwidth kernels [e.g. 32, 33] and dynamics adapted kernels [e.g. 34, 12]. Algorithm 1 does not specify the kernel, and any RKHS-like kernel would be sufficient whose associated RKHS is dense in $C(X)$.

References.

- [1] J. Li and L. Tran. Nonparametric estimation of conditional expectation. *J. Stat. Plann. Inference*, 139(2):164–175, 2009.
- [2] V. Duval, J. Aujol, and Y. Gousseau. On the parameter choice for the non-local means, 2010.

- [3] I. Frosio and J. Kautz. Statistical nearest neighbors for image denoising. *IEEE Trans. Image Process.*, 28(2):723–738, 2018.
- [4] T. Hastie and W. Stuetzle. Principal curves. *J. Amer. Stat. Assoc.*, 84(406):502–516, 1989.
- [5] S. Gerber and R. Whitaker. Regularization-free principal curve estimation. *J. Mach. Learning Res.*, 14(1):1285–1302, 2013.
- [6] L. Song, J. Huang, A. Smola, and K. Fukumizu. Hilbert space embeddings of conditional distributions with applications to dynamical systems. In *Proceedings of the 26th Annual International Conference on Machine Learning*, pages 961–968, 2009.
- [7] M. Mihcak, I. Kozintsev, K. Ramchandran, and P. Moulin. Low-complexity image denoising based on statistical modeling of wavelet coefficients. *IEEE Signal Process. Letters*, 6(12):300–303, 1999.
- [8] A. Hamza and H. Krim. Image denoising: A nonlinear robust statistical approach. *IEEE Trans. Signal Process.*, 49(12):3045–3054, 2001.
- [9] Z. Lu and X. Chen. Spatial nonparametric regression estimation: Non-isotropic case. *Acta Math. Appl. Sinica*, 18(4):641–656, 2002.
- [10] M. Hallin, Z. Lu, and L. Tran. Local linear spatial regression. *Anna. Stat.*, 32(6):2469–2500, 2004.
- [11] S. Steckley et al. A kernel approach to estimating the density of a conditional expectation. In *WINTER SIMULATION CONFERENCE*, volume 1, pages 383–391, 2003.
- [12] S. Das and D. Giannakis. Delay-coordinate maps and the spectra of Koopman operators. *J. Stat. Phys.*, 175:1107–1145, 2019.
- [13] S. Das and D. Giannakis. Koopman spectra in reproducing kernel Hilbert spaces. *Appl. Comput. Harmon. Anal.*, 49:573–607, 2020.
- [14] D. Giannakis and S. Das. Extraction and prediction of coherent patterns in incompressible flows through space-time Koopman analysis. *Phys. D*, 402:132211, 2019.
- [15] S. Das, D. Giannakis, and E. Szekely. An information-geometric approach for feature extraction in ergodic dynamical systems, 2020.
- [16] S. Mustavee, S. Das, and S. Agarwal. Data-driven discovery of quasiperiodically driven dynamics, 2023.
- [17] S. Das, S. Mustavee, S. Agarwal, and S. Hassan. Koopman-theoretic modeling of quasiperiodically driven systems: Example of signalized traffic corridor. *IEE Trans. SMC Sys.*, 53:1–11, 2023.
- [18] D. Giannakis, S. Das, and J. Slawinska. Reproducing kernel Hilbert space compactification of unitary evolution groups. *Appl. Comput. Harmon. Anal.*, 54:75–136, 2021.
- [19] R Coifman and S Lafon. Diffusion maps. *Appl. Comput. Harmon. Anal.*, 21:5–30, 2006.
- [20] N. Trillos and D. Slepčev. A variational approach to the consistency of spectral clustering. *Appl. Comput. Harmon. Anal.*, 45(2):239–281, 2018.
- [21] T. Berry, S. Das, D. Giannakis, and R. Vaughn. Spectral convergence of kernel integral operators, 2021. in preparation.

- [22] T. Berry and T. Sauer. Local kernels and the geometric structure of data. *Appl. Comput. Harmon. Anal.*, 40:439–469, 2016.
- [23] U. von Luxburg, M. Belkin, and O. Bousquet. Consistency of spectral clustering. *Ann. Stat.*, 26(2):555–586, 2008.
- [24] M. Hein, JY. Audibert, and U. Von Luxburg. From graphs to manifolds—weak and strong pointwise consistency of graph Laplacians. In *International Conference on Computational Learning Theory*, pages 470–485. Springer, 2005.
- [25] R. Vaughn, T. Berry, and H. Antil. Diffusion maps for embedded manifolds with boundary with applications to pdes, 2019.
- [26] V. Paulsen. An introduction to the theory of reproducing kernel Hilbert spaces, 2016.
- [27] M. Mollenhauer and P. Koltai. Nonparametric approximation of conditional expectation operators, 2020.
- [28] S. Das and D. Giannakis. Reproducing kernel Hilbert algebras on compact Lie groups. *J. Funct. Anal. Appl.*, 29, 2023.
- [29] A. Narayan, L. Yan, and T. Zhou. Optimal design for kernel interpolation: Applications to uncertainty quantification. *J. Comput. Phys.*, 430:110094, 2021.
- [30] R. Baraniuk and D. Jones. A signal-dependent time-frequency representation: optimal kernel design. *IEEE Trans. Signal Process.*, 41(4):1589–1602, 1993.
- [31] K. Crammer, J. Keshet, and Y. Singer. Kernel design using boosting. *Adv. Neural Inf Process. Sys.*, 15, 2002.
- [32] J. Fan and I. Gijbels. Data-driven bandwidth selection in local polynomial fitting: variable bandwidth and spatial adaptation. *J. Royal Stat. Soc. B*, 57(2):371–394, 1995.
- [33] T. Berry and J. Harlim. Variable bandwidth diffusion kernels. *Appl. Comput. Harmon. Anal.*, 40(1):68–96, 2016.
- [34] D. Giannakis. Dynamics-adapted cone kernels. *SIAM J. Appl. Dyn. Sys.*, 14(2):556–608, 2015.